Asymmetric transverse-load characteristics and polarization dependence of long-period fiber gratings written by a focused CO_2 laser

Yiping Wang,[1,2,*] Dong Ning Wang,[1] Wei Jin,[1] and Yunjiang Rao[3]

[1]Department of Electrical Engineering, The Hong Kong Polytechnic University, Kowloon, Hong Kong, China
[2]State Key Laboratory of Advanced Optical Communication Systems and Networks, Shanghai Jiao Tong University, Shanghai 200240, China
[3]School of Communication and Information Engineering, University of Electronic Science and Technology of China, Chengdu 610054, China

*Corresponding author: ypwang@china.com

Received 10 January 2007; accepted 16 February 2007;
posted 2 March 2007 (Doc. ID 78883); published 15 May 2007

Asymmetric transverse-load characteristics and the polarization dependence of long-period fiber gratings (LPFGs) written by high-frequency CO_2 laser pulses are investigated in detail. It is demonstrated that the resonant wavelength is dependent on the direction of the applied force and on the polarization state of the input light; however, the coupling strength is independent of these parameters. When a transverse load is applied along different orientations of the LPFG, the resonant wavelength may be shifted toward the longer wavelength, the shorter wavelength, or hardly shifted, whereas the absolute value of peak transmission attenuation is linearly decreased with an increase of the applied transverse load, with almost no sensitivity to the load direction. These unique transverse-load characteristics and the polarization dependence are due to the load-induced birefringence that leads to the rotation of optical principal axes in the LPFG. © 2007 Optical Society of America

OCIS codes: 060.2370, 060.2340, 050.2770.

1. Introduction

The long period fiber grating (LPFG) is a promising passive optical fiber device and has been widely used in the field of optical fiber communications and sensors [1–3]. Various techniques for fabricating LPFGs, e.g., ultraviolet (UV) laser exposure [1,2], CO_2 laser irradiation [4–6], electric arc discharge [7,8], etched corrugation [9,10], and mechanical microbends [11,12], have been proposed and demonstrated. The LPFGs obtained exhibit various mechanical characteristics due to different fabrication mechanisms. As reported by some of us [13,14] and by Van Wiggeren [15], the torsion and the bend characteristics of CO_2-laser-induced LPFGs depend strongly on the twist and the bend directions, respectively. In contrast, the mechanical characteristics of the LPFGs written by other techniques, such as UV laser exposure [16,17] and etched corrugation [9,10], are independent of the twist and the bend direction.

The transverse-load characteristic is one of the most important mechanical features of LPFGs. Liu *et al.* [18] and Zhang *et al.* [19] reported the transverse-load characteristics of UV-laser-induced LPFGs in photosensitive optical fiber and demonstrated that the loss peak of the LPFG was split into two subpeaks with the increased transverse load. The high-frequency CO_2 laser pulse technique is a promising method for LPFG fabrication, in which single-side irradiation with a CO_2 laser induced an asymmetric index profile within the cross section of the LPFG [5,15,20]. As a result, the LPFG obtained exhibits unique mechanical features, such as the torsion and the bend characteristics reported previously [13,14]. In Ref. [5] the responses of the CO_2-laser-induced LPFGs to the applied transverse load were briefly described.

0003-6935/07/163079-08$15.00/0

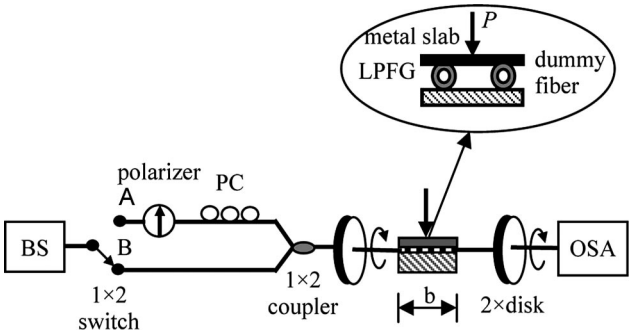

Fig. 1. Experimental setup for testing transverse-load characteristics and polarization dependence of the LPFGs. BS, broadband source; PC, polarization controller; OSA, optical spectral analyzer.

In this paper the unique transverse-load characteristics and polarization dependence of the CO_2-laser-induced LPFGs are investigated in detail by use of experiments and the optical principal axes' rotation resulting from the load-induced birefringence in the LPFGs.

2. Experimental Setup

Figure 1 illustrates the experimental setup for testing transverse-load characteristics and the polarization dependence of LPFGs fabricated by high-frequency CO_2 laser pulses in a conventional single-mode fiber. A broadband source with a center wavelength of 1550 nm and an optical spectrum analyzer (HP 86140A) with a wavelength resolution of 0.01 nm are employed to observe the transmission spectrum evolution. The 1×2 optical switch can be switched to port A or B to test the transverse-load characteristics or the polarization dependence of the LPFGs, respectively. The polarizer transforms the output of the broadband source into the linear polarized light. Then the state of polarization (SOP) of the polarized light can be adjusted by the polarization controller (Agilent 11896A). Two ends of the fiber with a tested LPFG in the middle are mounted on the centers of the two rotatable disks. Thus, when the two disks are rotated synchronously, the tested LPFG is turned around the axis of the fiber to test the responses of the LPFG to the transverse loads from different directions. The tested LPFG and a dummy fiber of the same type are laid between two flat metal slabs. A load, P, is applied step by step to the top metal slab. The weight of the top metal slab is 1.47 N, and the length of the loaded segment in the LPFG $b = 0.02$ m. Thus the actual transverse load on the unit length of LPFG is $(P + 1.47)/2b$.

3. Transverse-Load Characteristics of the LPFG

During the first experiment, the optical switch in Fig. 1 was connected to port B. The tested LPFG was written by focused high-frequency CO_2 laser pulses in Corning SMF-28 fiber [5], with 55 grating periods and a grating pitch of 500 μm. When the LPFG was in the load-free state at room temperature, its resonant wavelength and peak transmission attenuation were 1530.82 nm and −25.075 dB, respectively. When a weight $P = 31.36$ N was applied to the top metal slab, i.e., when a transverse load of 820.75 N m^{-1} was applied to the LPFG, the changes of the resonant wavelength and the peak transmission attenuation were measured by the optical spectrum analyzer. Then the LPFG was turned around its axis by means of two disks rotating synchronously with an angle of $\theta = 20°$, and the same transverse load of 820.75 N m^{-1} was applied to the LPFG again. The process was repeated until the total rotation angle of the LPFG was increased to 360°. Note that, each time before the LPFG was rotated, the weight and the top metal slab were removed. Consequently, a series of responses of the LPFG to the transverse load from different directions within the range of 0°–360° were tested with an angle step of 20°. As shown in Fig. 2(a), the LPFG's resonant wavelength is shifted toward the longer wavelength, i.e., is redshifted, when the transverse load is applied along some orientations, e.g., $0° \rightarrow \sim 45°$, $\sim 135° \rightarrow \sim 225°$, and $\sim 315° \rightarrow 360°$, of the fiber section where the LPFG is located, as shown in Fig. 2(c). In contrast, the LPFG's resonant wavelength is shifted toward the shorter wavelength, i.e., is blueshifted, when the transverse load is applied along other orientations, e.g., $\sim 45° \rightarrow \sim 135°$ and $\sim 225° \rightarrow \sim 315°$, of the

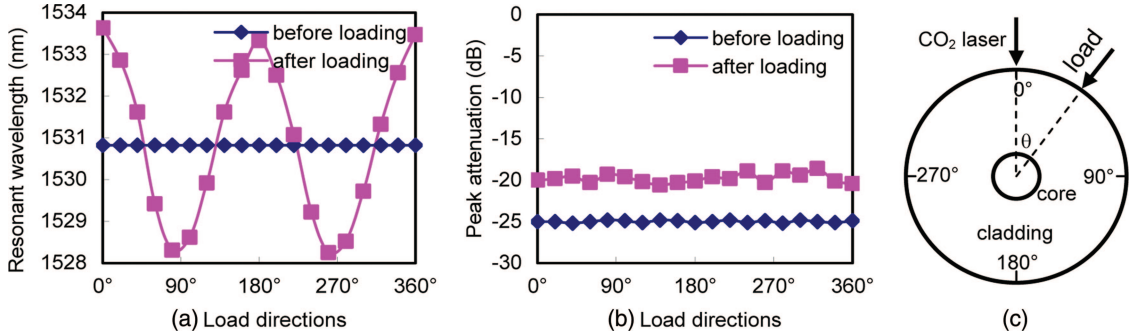

Fig. 2. (Color online) (a) Resonant wavelength and (b) peak transmission attenuation of the CO_2-laser-induced LPFG before and after a constant transverse load of 820.75 N m^{-1} is applied along different orientations θ of the fiber section where the LPFG is located, as shown in (c), where the direction of CO_2 laser irradiation during LPFG fabrication is defined as the 0° orientation at the circle of the LPFG.

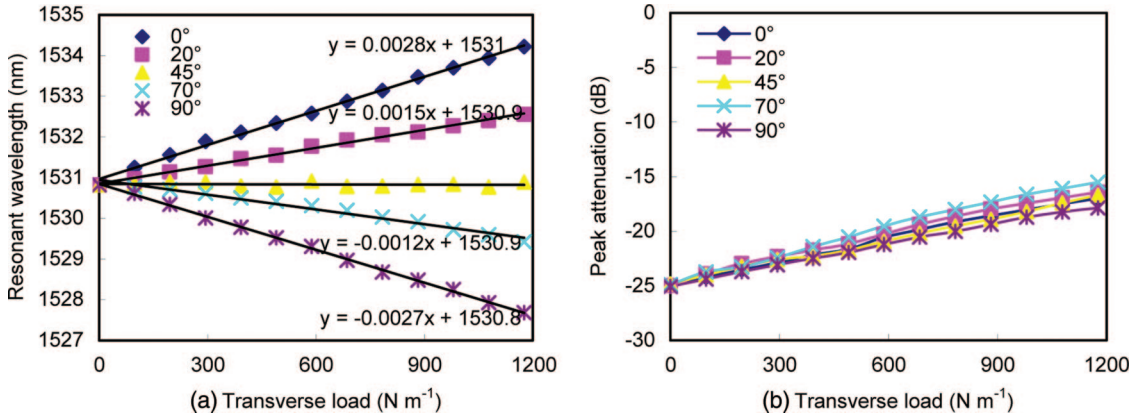

Fig. 3. (Color online) (a) Resonant wavelength and (b) peak transmission attenuation of the CO_2-laser-induced LPFG as functions of the transverse load applied along orientations 0°, 20°, 45°, 70°, and 90° of the LPFG.

LPFG. It can be seen from Fig. 2 that, although a constant transverse load is applied, the resonant wavelength shifts, corresponding to the load from different directions, are different. For example, within the range between 0° and 180°, for the load direction of 0°, the redshifted resonant wavelength is 2.81 nm; for the load direction of ~90°, the blueshifted resonant wavelength is −2.61 nm; for load directions of ~45° and ~135°, the resonant wavelength is hardly shifted by the transverse load. Therefore the load sensitivities of the resonant wavelength of the CO_2-laser-induced LPFG strongly depend on the load directions. As shown in Fig. 2(b), the changes of the peak transmission attenuation of the LPFG become similar after a constant transverse load of 820.75 N m^{-1} is applied along different orientations of the LPFG. In other words, the load-induced changes of the peak transmission attenuation of the CO_2-laser-induced LPFG are independent of the load directions.

During the second experiment, as shown in Fig. 3, a transverse load was applied along several orientations of 0°, 20°, 45°, 70°, and 90°, respectively, of the LPFG with a load step of 98 N m^{-1}. As shown in Fig. 3(a), the load sensitivities of the resonant wavelength for different load directions are different. For instance, the resonant wavelength is insensitive to the transverse load at the load direction of 45°, where the maximum wavelength shift is less than 0.1 nm. With the increase of the transverse load applied along the orientations of 0° and 20°, the resonant wavelength is linearly shifted toward the longer wavelength with a sensitivity of 0.0028 and 0.0015 nm (N m^{-1})$^{-1}$, respectively, whereas, with the increase of the transverse load applied along the orientations of 70° and 90°, the resonant wavelength is linearly shifted toward the shorter wavelength with a sensitivity of −0.0012 and −0.0027 nm (N m^{-1})$^{-1}$, respectively. As shown in Fig. 3(b), the absolute value of the peak transmission attenuation of the LPFG is linearly decreased with the increase of the transverse load for each load direction, and the load sensitivities of the peak transmission attenuation for different load directions are only about 0.007 dB (N m^{-1})$^{-1}$. Figure 4 illustrates transmission spectrum evolution of the CO_2-laser-induced LPFG when transverse loads of 0, 196, 392, 588, and 784 N m^{-1} are each applied along the 0° orientation of the LPFG. It can be seen from Fig. 4 that, with the increase of the transverse load, the resonant wavelength is shifted from 1530.82 toward 1533.14 nm, and the peak transmission attenuation is changed from −25.075 to −19.158 dB.

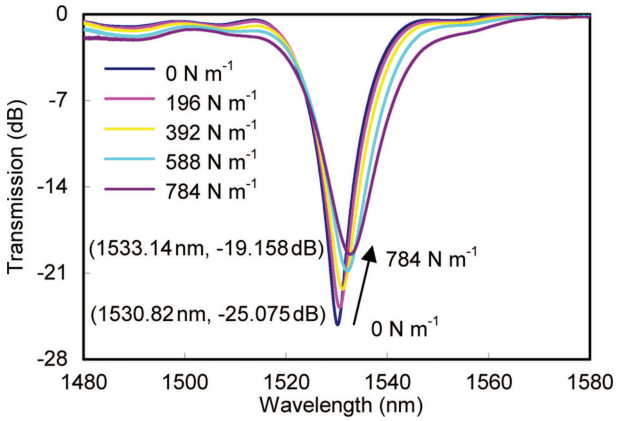

Fig. 4. (Color online) Transmission spectrum evolution of the CO_2-laser-induced LPFG when transverse loads of 0, 196, 392, 588, and 784 N m^{-1} are each applied along the 0° orientation of the LPFG.

4. Polarization Dependence of the LPFG

During the third experiment, the optical switch in Fig. 1 was connected to port A to test the polarization dependence of the CO_2-laser-induced LPFG. Another LPFG written by high-frequency CO_2 laser pulses was employed. When the LPFG was in the load-free state and at room temperature, its resonant wavelength and peak transmission attenuation were 1528.52 nm and −19.694 dB, respectively. The top metal slab illustrated in Fig. 1 was laid on one side, with an orientation of 105°, of the LPFG and a weight of 31.36 N was applied to the top metal

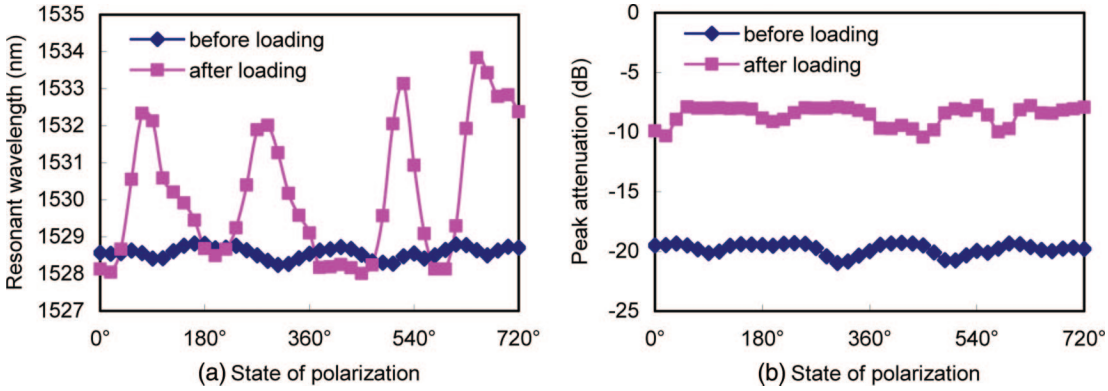

Fig. 5. (Color online) (a) Resonant wavelength and (b) peak transmission attenuation as functions of the SOP of the input light before and after a transverse load of 820.75 N m^{-1} is applied along the 105° orientation of the LPFG. *X* coordinates in this figure and in Fig. 6 illustrate the accumulative angular adjustment of four fiber loops in the polarization controller, i.e., the adjustment of the SOP of the transmitted light.

slab. That is, a transverse load of 820.75 N m^{-1} was applied along a special orientation, i.e. 105°, of the LPFG. Then the SOP of the input light of the LPFG was adjusted by the polarization controller. As shown in Fig. 5(a), during the adjustment of the SOP of the input light, the maximum changes of the resonant wavelength are 0.5 and 5.5 nm, respectively, before and after the transverse load is applied. That is, the polarization dependences of the resonant wavelength of the LPFG with and without a transverse load are different. As shown in Fig. 5(b), although the LPFG's peak transmission attenuation is changed from −19.694 to −9 dB after the transverse load is applied, its fluctuation is still ~2 dB during the adjustment of the SOP of the input light. There are four fiber loops in the polarization controller (Agilent 11896A). The transmitted signal that enters the polarization controller passes through the four-fiber-loop assembly. The dimensions of each loop have been optimized to approximate a quarter-wave retarder response over the polarization controller's specified wavelength range.

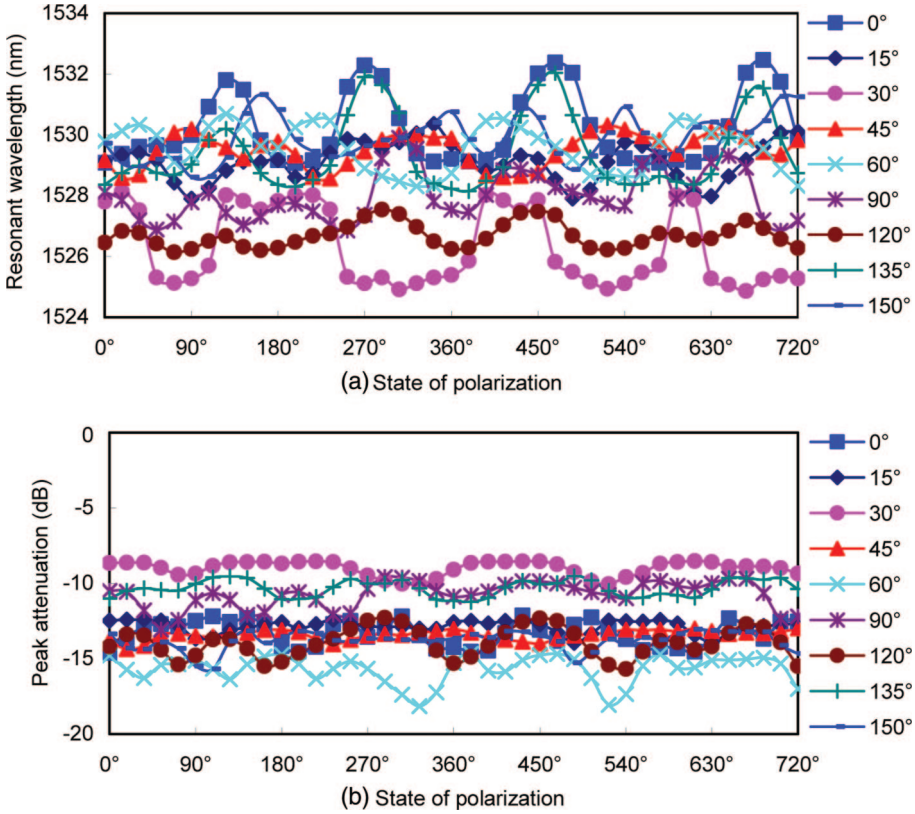

Fig. 6. (Color online) Polarization dependence of (a) resonant wavelength and (b) peak transmission attenuation after a transverse load of 820.75 N m^{-1} is applied in turn along orientations 0°, 15°, 30°, 45°, 60°, 90°, 120°, 135°, and 150° of the LPFG.

Complete and continuous polarization adjustment can be achieved by independently adjusting each fiber loop over an angular range of 180°. In our experiments, the adjustments were made manually by using the four knobs in the front panel, where each knob corresponds to one internal fiber loop.

During the fourth experiment, a constant transverse load of 820.75 N m^{-1} was applied in turn along the orientations 0°, 15°, 30°, 45°, 60°, 90°, 120°, 135°, and 150° of the LPFG, and then the polarization dependence of the LPFG was tested by the process described in the third experiment. As shown in Fig. 6(a), although a constant transverse load was applied along each orientation of the LPFG, the relevant polarization dependence of resonant wavelength at different load directions were different. For instance, when the transverse load is applied along the orientation of 0° or 45°, the maximum changes of the resonant wavelength are ~5 and ~2 nm, respectively, while the SOP of the input light is adjusted. As shown in Fig. 6(b), when a constant transverse load is applied, the polarization dependence of peak transmission attenuation, corresponding to different load directions, are about 2 dB.

5. Analysis and Discussion

A. Load-Induced Rotation of Principal Optical Axes in the Fiber

The load-induced distortion and strain create a new linear birefringence in the optical fiber due to the photoelastic effect, which leads the original optical principal axes of the fiber to rotate gradually toward the load direction with the increase of transverse load and to be finally aligned with the load direction [21,22]. The load-induced birefringence first has to overcome the original birefringence to rotate the optical principal axes of the fiber. Thus the higher the original birefringence of the fiber is, the larger the transverse load necessary to overcome the original birefringence is. As a result, the smaller the original birefringence in the fiber is, the more sensitive the load-induced rotation of the optical principal axes is. In addition, the sensitivity of optical principal axes rotation induced by the load depend strongly on the angle, α, between the transverse load and the original optical principal axes of the fiber [21,22]. In the case in which the load direction is parallel or normal to the original optical principal axes of the fiber, i.e., $\alpha = 0°$ or 90°, although a new birefringence is induced by the applied transverse load on the fiber, the optical principal axes hardly rotate. In contrast, in the case $\alpha = 45°$ the rotation of the optical principal axes shows the largest sensitivity to the transverse load.

The refractive indexes corresponding to the original fast and slow optical principal axes in the fiber are defined as n_f and n_s, respectively. After a transverse load is applied to the fiber, the rotation angle, $\Delta\alpha$, of the optical principal axes and the new refractive indexes, $n_{f'}$ and $n_{s'}$, corresponding to the new fast and slow optical principal axes, respectively, can be given by [21,22]

$$\tan \Delta\alpha = \frac{b}{d + \Psi}, \tag{1}$$

$$\frac{1}{n_{f'}^2} = \Phi + \Psi, \tag{2}$$

$$\frac{1}{n_{s'}^2} = \Phi - \Psi, \tag{3}$$

where

$$\Phi = \frac{a + c}{2} = \frac{1}{2}\left[\frac{1}{n_f^2} + \frac{1}{n_s^2} + (p_1 + p_2)(e_{xx} + e_{yy}) + 2p_2 e_{zz}\right],$$

$$\Psi = \sqrt{d^2 + b^2},$$

$$d = \frac{a - c}{2} = \frac{1}{2}\left[\frac{1}{n_f^2} - \frac{1}{n_s^2} + (p_1 - p_2)(e_{xx} - e_{yy})\cos 2\alpha\right],$$

$$a = \frac{1}{n_f^2} + \Delta K_{ff}, \qquad b = \frac{1}{2}\Delta K_{sf}, \qquad c = \frac{1}{n_s^2} + \Delta K_{ss},$$

where p_1 and p_2 are the components of the transverse load, ΔK_{ff}, ΔK_{sf}, and ΔK_{ss} are the changes of the optical impermeability tensor that are due to the photoelastic effect in the fiber, and e_{xx} and e_{yy} are the strain components of the fiber that are due to the transverse load.

B. Transverse Characteristics and Polarization Dependence of the LPFG

The single-side irradiation of CO_2 laser results in an asymmetric index profile within the cross section of the CO_2-laser-induced LPFGs [5,15,23]. The index modulation on the laser incident side of the fiber is larger than that on the laser output side of the fiber. Consequently, a linear birefringence exists in the CO_2-laser-induced LPFG. The fundamental core mode, LP_{01}, in the CO_2-laser-induced LPFG with a linear birefringence can be divided into two normal polarization modes, i.e., $LP_{01\text{-}f}$ and $LP_{01\text{-}s}$. Thus the propagation constants, β_f and β_s, of the two normal polarization modes in the CO_2-laser-induced LPFG can be defined as

$$\beta_f = \frac{2\pi}{\lambda} n_f, \tag{4}$$

$$\beta_s = \frac{2\pi}{\lambda} n_s. \tag{5}$$

The combination of the propagation constants, β_f and β_s, of the two polarization modes determines the propagation constant, β_{01}, of the fundamental core mode. The changes of β_f and β_s resulting from the

increase or decrease of n_f and n_s, will inevitably affect the mode coupling in the LPFG, which will change the resonant wavelength and the peak transmission attenuation of the LPFG.

After a transverse load is applied to the LPFG, a new linear birefringence is induced in the LPFG, which rotates the original optical principal axes of the LPFG. Thus the refractive indexes corresponding to the optical principal axes in the LPFG change from n_f and n_s to $n_{f'}$ and $n_{s'}$, respectively, and

$$\beta_{f'} = \frac{2\pi}{\lambda} n_{f'} \neq \beta_f, \tag{6}$$

$$\beta_{s'} = \frac{2\pi}{\lambda} n_{s'} \neq \beta_s, \tag{7}$$

where $\beta_{f'}$ and $\beta_{s'}$ are the propagation constants of two normal polarization modes, corresponding to the new fast and slow optical principal axes, respectively, with a transverse load applied to the LPFG. The combination of $\beta_{f'}$ and $\beta_{s'}$ determines the propagation constant, β_{01}', of the fundamental core mode in the LPFG with a transverse load. Since $\beta_{f'} \neq \beta_f$ and $\beta_{s'} \neq \beta_s$, it follows that $\beta_{01}' \neq \beta_{01}$, i.e., the transverse load causes a change in the propagation constant of the fundamental core mode. Thus, the resonant wavelength and the peak transmission attenuation will be changed when a transverse load is applied to the CO_2-laser-induced LPFG. According to Eqs. (2) and (3), the load-induced refractive index change, Δn_f and Δn_s, is dependent on not only the value but also the direction of the transverse load. Thus the value and the direction of the transverse load applied to the LPFG determine the changes of the resonant wavelength and the peak transmission attenuation, as shown in Figs. 2 and 3.

The birefringence in the LPFG results from the LPFG's transmission characteristics that depend strongly on the SOP of the input light. The load-induced birefringence and the original birefringence in the LPFG are combined to form a new birefringence. As a result, the polarization dependence of the LPFG will be changed when a transverse load is applied to the LPFG. According to Eq. (1), the load-induced rotation of the optical principal axes is dependent on the value and the direction of the applied transverse load. Thus the polarization dependence of the LPFG with a transverse load is dependent on not only the value but also the direction of the transverse load. In other words, when a constant load is applied along different orientations of the LPFG, the polarization dependence of the resonant wavelength may be distinguishable, as shown in Fig. 6.

The stress-induced birefringence also affects the cladding mode, which implies that the cladding mode in the LPFG with a transverse load can be expressed as LP_{mn}^{x} and LP_{mn}^{y}. The coupling between the fundamental core mode and the cladding mode determines the transmission spectrum of the LPFG. When the load-induced birefringence is large enough, these two normal polarization modes, LP_{mn}^{x} and LP_{mn}^{y}, will cause the original attenuation peak be split into two subpeaks, as observed in the UV-laser-induced LPFGs [18,19]. In our experiments, when a large transverse load of 2940 N m^{-1} was applied to the CO_2-laser-induced LPFG, the original attenuation peak was also split into two subpeaks. However, when a small transverse load, e.g., 820.75 N m^{-1}, was applied, the original attenuation peak was just broadened, instead of being split into two subpeaks. All of the experiments described in Sections 2 and 3 were done under conditions for which the original attenuation peak of the LPFG was not split into two subpeaks.

C. Load Direction Dependence of the Transverse-Load Characteristics of the LPFG

As shown in Fig. 7, the resonant wavelength is redshifted when the transverse load is applied to the "+" orientations of the LPFG. And the resonant wavelength is blueshifted when the transverse load is applied along the "−" orientations. Furthermore, the redshifted resonant wavelength has maximum sensitivity to the transverse load applied along the orientation parallel to the direction of CO_2 laser irradiation; the blueshifted resonant wavelength has maximum sensitivity to the transverse load applied along the orientation normal to the direction of CO_2 laser irradiation; the resonant wavelength has almost no sensitivity (or the minimum sensitivity) to the transverse load when the angle between the direction of the transverse load and that of the CO_2 laser irradiation is 45°, 135°, 225°, or 315°. The center of the refractive index ellipse within the cross section of the CO_2-laser-induced LPFG usually fails to exactly overlap the geometric center of the optical fiber. As a result, the load directions, corresponding to the

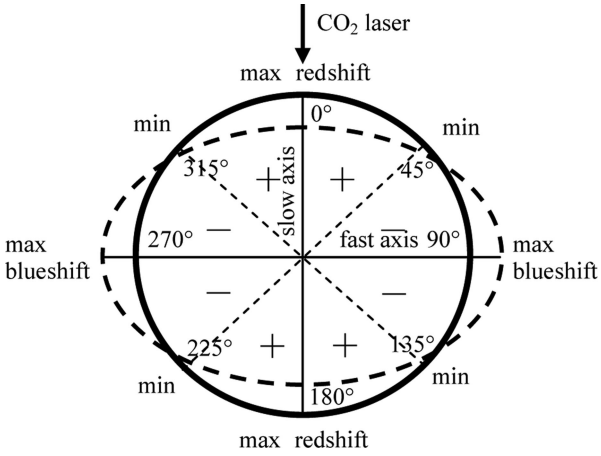

Fig. 7. Schematic diagram of the load sensitivities of the resonant wavelength when a transverse load is applied along different orientations of the CO_2-laser-induced LPFG. The dashed ellipse illustrates the refractive index ellipse induced by the asymmetric index profile within the cross section of the LPFG, where the longer and shorter axes are defined as the fast and slow axes, respectively, and the direction of CO_2 laser irradiation is defined as the 0° orientation of the LPFG.

maximum redshift sensitivity, the maximum blueshift sensitivity, and the minimum shift sensitivity of the resonant wavelength, are not exactly at the orientations marked in Fig. 7. In other words, they are just near the orientations, 0° and 180°, 90° and 270°, and 45°, 135°, 225°, and 315°, of the LPFG, respectively, as shown in Fig. 2(a).

The total birefringence, consisting of the inherent birefringence and the load-induced birefringence, in the LPFG varies periodically with the direction of the applied transverse load. Whether the load-induced birefringence weakens or enhances the birefringence in the LPFG with an inherent birefringence depends on the direction of the applied transverse load. Thus the total birefringence in the LPFG is distinguishable when a constant transverse load is applied along different orientations of the LPFG. Hence the mode coupling between the fundamental core mode and the cladding mode is varied. As a result, the transverse-load characteristics of the LPFG depend strongly on the direction of the applied transverse load. If the direction of the applied transverse load is parallel or normal to the CO_2 laser incident direction, the longer axis and shorter axis of the LPFG with opposite strains, i.e., the stretch strain and the shrink strain, cause the refractive indexes, n_f and n_s, to change in opposite directions. Thus the transmission constants, β_f and β_s, of the two normal polarization modes also change in opposite directions, which leads to a maximum change in the transmission constant, β_{01}, of the fundamental core mode. As a result, the mode coupling between the fundamental core mode and the cladding mode obviously change. Also, the LPFG's resonant wavelength has maximum sensitivity to the transverse load that is parallel or normal to the direction of CO_2 laser irradiation.

If the direction of the applied transverse load is parallel to the direction of CO_2 laser irradiation, the longer axis has the stretch strain, and the shorter axis has the shrink strain. If the direction of the transverse load is normal to the direction of CO_2 laser irradiation, the longer axis has the shrink strain, and the shorter axis has the stretch strain. Thus when the transverse load direction is parallel or normal to the direction of CO_2 laser irradiation, the load-induced changes of the mode coupling between the fundamental core mode and the cladding mode are opposite, which causes the resonant wavelength to be shifted toward the opposite direction. If the angle between the direction of the transverse load and that of the CO_2 laser irradiation is 45°, 135°, 225°, or 315°, the LPFG's longer and shorter axes have similar strain. Consequently, the change of n_f is nearly equal to that of n_s, and the change of β_f is nearly equal to that of β_s, which induces only a similar change in the transmission constant of β_{01}, and the mode coupling between the fundamental core mode and the cladding mode hardly changes. Thus the LPFG's resonant wavelength has almost no sensitivity to the transverse load when the angle between the direction of the applied transverse load and that of the CO_2 laser irradiation is 45°, 135°, 225°, or 315°.

6. Conclusions

For the CO_2-laser-induced LPFG, the transverse-load characteristics of the resonant wavelength are dependent on the direction of the applied transverse load, whereas those of the peak transmission attenuation are independent of the direction of the applied transverse load. The redshifted or blueshifted resonant wavelength has maximum sensitivity to the transverse load applied along the orientation that is parallel or normal to the direction of CO_2 laser irradiation of the LPFG. The resonant wavelength has almost no sensitivity to the applied transverse load when the angle between the direction of the applied transverse load and that of the CO_2 laser irradiation is 45°, 135°, 225°, or 315°. The absolute value of the peak transmission attenuation of the CO_2-laser-induced LPFG decreases linearly with the increase of the transverse load applied along every orientation of the LPFG. The polarization dependence of the resonant wavelength can be changed by the transverse load, which is dependent on the direction of the applied transverse load, whereas the polarization dependence of the peak transmission attenuation is hardly affected by the transverse load. Obviously, linear birefringence exists in the LPFG written by high-frequency CO_2-laser pulses. These unique transverse-load characteristics of the CO_2-laser-induced LPFG can be used in the field of optical fiber communications and optical fiber sensors.

This work is supported by the research grants of the Hong Kong Polytechnic University in a Postdoctoral Research Fellowship scheme (ID G-YX51) and the National Science Foundation of China (ID 60507013).
D. N. Wang's email is eednwang@polyu.edu.hk.

References

1. A. M. Vengsarkar, P. J. Lemaire, J. B. Judkins, V. Bhatia, T. Erdogan, and J. E. Sipe, "Long-period fiber gratings as band-rejection filters," J. Lightwave Technol. **14,** 58–65 (1996).
2. V. Bhatia and A. M. Vengsarkar, "Optical fiber long-period grating sensors," Opt. Lett. **21,** 692–694 (1996).
3. A. D. Kersey, M. A. Davis, H. J. Patrick, M. LeBlanc, K. P. Koo, C. G. Askins, M. A. Putnam, and E. J. Friebele, "Fiber grating sensors," J. Lightwave Technol. **15,** 1442–1463 (1997).
4. D. D. Davis, T. K. Gaylord, E. N. Glytsis, S. G. Kosinski, S. C. Mettler, and A. M. Vengsarkar, "Long-period fibre grating fabrication with focused CO_2 laser pulses," Electron. Lett. **34,** 302–303 (1998).
5. Y. J. Rao, Y. P. Wang, Z. L. Ran, and T. Zhu, "Novel fiber-optic sensors based on long-period fiber gratings written by high-frequency CO_2 laser pulses," J. Lightwave Technol. **21,** 1320–1327 (2003).
6. Y.-P. Wang, D. N. Wang, W. Jin, Y.-J. Rao, and G.-D. Peng, "Asymmetric long period fiber gratings fabricated by use of CO_2 laser to carve periodic grooves on the optical fiber," Appl. Phys. Lett. **89,** 151105-3 (2006).
7. G. Rego, O. Okhotnikov, E. Dianov, and V. Sulimov, "High-temperature stability of long-period fiber gratings produced using an electric arc," J. Lightwave Technol. **19,** 1574–1579 (2001).
8. I. K. Hwang, S. H. Yun, and B. Y. Kim, "Long-period fiber gratings based on periodic microbends," Opt. Lett. **24,** 1263–1265 (1999).
9. C. Y. Lin, L. A. Wang, and G. W. Chern, "Corrugated long-

period fiber gratings as strain, torsion, and bending sensors," J. Lightwave Technol. **19,** 1159–1168 (2001).
10. C. Y. Lin and L. A. Wang, "A wavelength- and loss-tunable band-rejection filter based on corrugated long-period fiber grating," IEEE Photon. Technol. Lett. **13,** 332–334 (2001).
11. S. Savin, M. J. F. Digonnet, G. S. Kino, and H. J. Shaw, "Tunable mechanically induced long-period fiber gratings," Opt. Lett. **25,** 710–712 (2000).
12. J. Y. Cho and K. S. Lee, "A birefringence compensation method for mechanically induced long-period fiber gratings," Opt. Commun. **213,** 281–284 (2002).
13. Y. P. Wang, J. P. Chen, and Y. J. Rao, "Torsion characteristics of long-period fiber gratings induced by high-frequency CO_2 laser pulses," J. Opt. Soc. Am. B **22,** 1167–1172 (2005).
14. Y. P. Wang and Y. J. Rao, "A novel long period fiber grating sensor measuring curvature and determining bend-direction simultaneously," IEEE Sens. J. **5,** 839–843 (2005).
15. G. D. VanWiggeren, T. K. Gaylord, D. D. Davis, E. Anemogiannis, B. D. Garrett, M. I. Braiwish, and E. N. Glytsis, "Axial rotation dependence of resonances in curved CO_2-laser-induced long-period fibre gratings," Electron. Lett. **36,** 1354–1355 (2000).
16. H. J. Patrick, "Self-aligning, bipolar bend transducer based on long period grating written in eccentric core fibre," Electron. Lett. **36,** 1763–1764 (2000).
17. Y. Liu, L. Zhang, J. A. R. Williams, and I. Bennion, "Optical bend sensor based on measurement of resonance mode splitting of long-period fiber grating," IEEE Photon. Technol. Lett. **12,** 531–533 (2000).
18. Y. Liu, L. Zhang, and I. Bennion, "Fibre optic load sensors with high transverse strain sensitivity based on long-period gratings in B/Ge co-doped fibre," Electron. Lett. **35,** 661–663 (1999).
19. L. Zhang, Y. Liu, L. Everall, J. A. R. Williams, and I. Bennion, "Design and realization of long-period grating devices in conventional and high birefringence fibers and their novel applications as fiber-optic load sensors," IEEE J. Sel. Top. Quantum Electron. **5,** 1373–1378 (1999).
20. B. H. Kim, Y. Park, T. J. Ahn, D. Y. Kim, B. H. Lee, Y. Chung, U. C. Paek, and W. T. Han, "Residual stress relaxation in the core of optical fiber by CO_2 laser irradiation," Opt. Lett. **26,** 1657–1659 (2001).
21. J. Calero, S. P. Wu, C. Pope, S. L. Chuang, and J. P. Murtha, "Theory and experiments on birefringent optical fibers embedded in concrete structures," J. Lightwave Technol. **12,** 1081–1091 (1994).
22. J. Calero, S. L. Chuang, and J. P. Murtha, "Anomalous optical transmission due to strain-induced optical axis rotation in optical fibers embedded in concrete," Smart Mater. Struct. **7,** 12–22 (1998).
23. H. S. Ryu, Y. Park, S. T. Oh, Y. J. Chung, and D. Y. Kim, "Effect of asymmetric stress relaxation on the polarization-dependent transmission characteristics of a CO_2 laser-written long-period fiber grating," Opt. Lett. **28,** 155–157 (2003).